Structure–Function Relationships in EF-Hand Ca^{2+}-Binding Proteins. Protein Engineering and Biophysical Studies of Calbindin D_{9k}†

Sara Linse,‡ Peter Brodin,§ Torbjörn Drakenberg,‡ Eva Thulin,‡ Peter Sellers,‡ Karin Elmdén,‡ Thomas Grundström,§ and Sture Forsén*,‡

Department of Physical Chemistry 2, Chemical Centre, Lund University, S-221 00 Lund, Sweden, and Unit of Applied Cell and Molecular Biology, University of Umeå, S-901 87 Umeå, Sweden

Received April 9, 1987; Revised Manuscript Received June 3, 1987

ABSTRACT: Genes encoding the minor A component of bovine calbindins D_{9k}—the smallest protein known with a pair of EF-hand calcium-binding sites—with amino acid substitutions and/or deletions have been synthesized and expressed in *Escherichia coli* and characterized with different biophysical techniques. The mutations are confined to the N-terminal Ca^{2+}-binding site and constitute Pro-20 → Gly (M1), Pro-20 → Gly and Asn-21 deleted (M2), Pro-20 deleted (M3), and Tyr-13 → Phe (M4). ^1H, ^{43}Ca, and ^{113}Cd NMR studies show that the structural changes induced are primarily localized in the modified region, with hardly any effects on the C-terminal Ca^{2+}-binding site. The Ca^{2+} exchange rate for the N-terminal site changes from 3 s^{-1} in the wild-type protein (M0) and M4 to 5000 s^{-1} in M2 and M3, whereas there is no detectable variation in the Ca^{2+} exchange from the C-terminal site. The macroscopic Ca^{2+}-binding constants have been obtained from equilibration in the presence of the fluorescent chelator 2-[[2-[bis(carboxymethyl)-amino]-5-methylphenoxy]methyl]-6-methoxy-8-[bis(carboxymethyl)amino]quinoline or by using a Ca^{2+}-selective electrode. The Ca^{2+} affinity of M4 was similar to that of M0, whereas the largest differences were found for the second stoichiometric step in M2 and M3. Microcalorimetric data show that the enthalpy of Ca^{2+} binding is negative (−8 to −13 kJ·mol^{-1}) for all sites except the N-terminal site in M2 and M3 (+5 kJ·mol^{-1}). The binding entropy is strongly positive in all cases. Cooperative Ca^{2+} binding in M0 and M4 was established through the values of the macroscopic Ca^{2+}-binding constants. Through the observed changes in the ^1H NMR spectra during Ca^{2+} titrations we could obtain ratios between site binding constants in M0 and M4. These ratios in combination with the macroscopic binding constants yielded the interaction free energy between the sites $\Delta\Delta G$ as −5.1 ± 0.4 kJ·mol^{-1} (M0) and <−3.9 kJ·mol^{-1} (M4). There is evidence (from ^{113}Cd NMR) for site–site interactions also in M1, M2, and M3, but the magnitude of $\Delta\Delta G$ could not be determined because of sequential Ca^{2+} binding.

The calcium messenger system plays a central role in mediating a variety of biological processes: cell division and growth, muscle contraction, secretion, ion transport, and the metabolic processes of glycogenolysis and gluconeogenesis. The detailed organization of this system is presently the subject of considerable scientific interest (Rasmussen, 1986a,b).

One of the links in the calcium messenger system is a class of highly homologous Ca^{2+}-binding proteins that undergo Ca^{2+}-dependent conformational changes and respond to transitory increases in intracellular Ca^{2+} ion concentrations. Well-known members of this class are calmodulin, skeletal and heart muscle troponins C (Klee et al., 1982; Manalan & Klee, 1984; McCubbin & Kay, 1980; Potter & Johnson, 1982), the S100 proteins, parvalbumin, and the 9k and 28k calbindins.[1] X-ray crystallographic data are presently available for four member proteins: carp parvalbumin (Kretsinger & Nockolds, 1973; Moews & Kretsinger, 1975), calf calbindin D_{9k} (Szebenyi et al., 1981; Szebenyi & Moffat, 1986), turkey and chicken skeletal muscle troponin C (Herzberg & James, 1985a,b; Sundralingam et al., 1985), and rat and cow calmodulin (Babu et al., 1985; Kretsinger & Weissman, 1986). These studies have conclusively shown that all the Ca^{2+}-binding sites are constructed in a similar fashion—colloquially termed "the EF hand" (Kretsinger & Nockolds, 1973). This structural unit is made up of two helices separated by a calcium-binding loop which is typically 12 amino acid residues long and is wrapped around the Ca^{2+} ion in such a way that the ion is roughly octahedrally coordinated with oxygen atoms. A second structural feature of these proteins is that pairs of EF hands rather than individual binding sites seem to be the functional unit. Interactions between the two Ca^{2+} sites in such functional domains have been observed spectroscopically, and cooperative Ca^{2+} binding is often found [for recent reviews, see Seamon and Kretsinger (1983), Forsén et al. (1986), Vogel and Forsén (1987), and Herzberg et al. (1986)]. Another striking property in this family of proteins is that the Ca^{2+}-binding constants range from about 10^5 M^{-1} to 10^9 M^{-1} with no obvious correlation with the nature and disposition of the ligands (Szebenyi & Moffat, 1976; Herzberg & James, 1985a,b). Little information is as yet available on the molecular details of the conformational changes that accompany Ca^{2+}-ion binding. It has, however, been suggested that the structural differences found in turkey troponin C between the C-terminal domain, which in the crystal studied contains two bound Ca^{2+} ions, and the N-terminal domain, in which no Ca^{2+} ions are bound under

† This work was supported by grants from the Swedish National Science Research Council (K-KU 2541-116).

* Correspondence should be addressed to this author.
‡ Lund University.
§ University of Umeå.

[1] By consensus among a large number of scientists working in the field of Ca^{2+}-binding proteins the vitamin D dependent 28k chicken intestinal calcium-binding protein (28k ICaBP) and the bovine and porcine calcium-binding protein (9k ICaBP) should now be referred to as calbindin 28k (or calbindin D_{28k}) and calbindin 9k (or calbindin D_{9k}), respectively (A. W. Norman, personal communication).

0006-2960/87/0426-6723$01.50/0

the conditions of crystallization, may represent these conformational changes (Herzberg et al., 1986).

In order to explore further the relationships between structure and function in the EF-hand class of Ca^{2+}-binding proteins, in particular the molecular nature of the Ca^{2+} binding and the site–site interaction, we have chosen to combine biophysical methods with the powerful tool of "site-directed mutagenesis" (Harris, 1982; Smith, 1982). The protein selected for this investigation is bovine calbindin D_{9k} (intestinal calcium-binding protein, ICaBP) or rather its "minor A" component obtained from the native protein by proteolytic removal of the two N-terminal amino acids (Fullmer & Wasserman, 1981). The small size of this protein (75 amino acids, M_r 8501) makes it particularly attractive for NMR spectroscopic studies. It has no cysteines, which simplifies handling of the protein solutions, and only one tyrosine, which facilitates the interpretation of static and time-resolved fluorescence data. The X-ray structure of the minor A form of calbindin D_{9k} has recently been refined to a resolution of 2.3 Å (Szebenyi & Moffat, 1986), and its overall features are similar to those of the Ca^{2+}-binding globular domains of parvalbumin, calmodulin, and troponin C. The Ca^{2+}-binding site in the C-terminal half of the molecule has the same fold as that in the archetypal EF hand whereas the site in the N-terminal half constitutes a variant hand in which the Ca^{2+} ligands are mostly peptide carbonyls.

In a recent publication we have described the design, synthesis, and expression in *Escherichia coli* of a gene encoding the minor A form of calbindin D_{9k} (Brodin et al., 1986). In the present paper we report the synthesis, expression, and characterization by different biophysical techniques of four mutant calbindins and compare their properties to those of the wild-type protein. In order to investigate the molecular details of the Ca^{2+} binding and site–site interaction, previously observed through NMR studies (Vogel et al., 1985), we have chosen to perturb one of the Ca^{2+}-binding sites. Thus all mutations are in the present work confined to the N-terminal Ca^{2+}-binding site ("the pseudo EF hand"), which has some unusual features as compared to a normal EF hand. There are two additional amino acids in the loop, and one of them is a proline. For the present we have studied the effects of either removing the proline or replacing it with glycine. One objective was to see if the effects of such localized changes would be confined to the Ca^{2+}-binding properties of the modified site only. Finally, we have replaced the single tyrosine with a phenylalanine in order to see if the hydrogen bond between Tyr-13 and Glu-35, which links the helices flanking the N-terminal site (Szebenyi & Moffat, 1981), influences the stability and Ca^{2+}-binding properties of the protein.

Materials and Methods

Definition of Mutant Proteins. A schematic outline of calbindin is shown in Figure 1. In the following, M0 designates the wild-type minor A form of bovine calbindin D_{9k} with an additional methionine residue at the N-terminus, while M1 through M4 designate the mutant proteins with the following modifications relative to M0: M1, Pro-20 → Gly; M2, Pro-20 → Gly and Asn-21 deleted; M3, Pro-20 deleted; M4, Tyr-13 → Phe. The numbering scheme of Fullmer and Wasserman (1981) is used throughout. Note that the N-terminal methionine is thereby given number zero.

The Ca^{2+}-binding sites are denoted with Roman numbers—I for the N-terminal site and II for the C-terminal site. The α-helices are denoted A–D, starting at the N-terminus.

Synthesis of Mutant Proteins. The synthesis and expression in *E. coli* of a gene encoding a protein identical with the minor

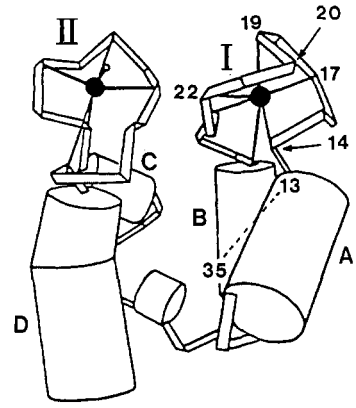

FIGURE 1: Schematic structure of calbindin 9k, after Szebenyi and Moffat (1983).

A form of bovine calbindin D_{9k} have been described previously (Brodin et al., 1986). In order to construct calbindins with substitutions and/or deletions of amino acids in the N-terminal half of the protein containing the pseudo-EF-hand calcium-binding loop, a 101 base pair segment of the gene, bordered with *Eco*RI and *Pst*I restriction sites and corresponding to the first 33 amino acids of the protein, was replaced with a polylinker made up from two oligonucleotides (Figure 2). The bordering sites in the polylinker were subsequently used for reassembling DNA segments coding for the N-terminal amino acids from a set of oligonucleotides (Brodin et al., 1986) with codon changes as follows. In M1 and M2, the Pro-20 codon, CCG, was replaced by the glycine codon, GGT; in addition, in M2 the Asn-21 codon, AAC, was deleted. M3 was constructed by deleting the Pro-20 codon, CCG. In M4 the Tyr-13 codon, TAC, was replaced by the phenylalanine codon, TTC.

The nucleotide sequences of the constructed DNA segments were confirmed by dideoxy sequencing. The genes were cloned into the expression vector pICB1 (Brodin et al., 1986). Synthesis of the protein variants was confirmed by SDS^2–polyacrylamide gel electrophoresis in the same way as previously described.

Purification of Mutant Proteins. The wild-type protein, M0, and the mutant proteins M1, M2, and M3 were purified as previously described (Brodin et al., 1986). The steps consisted of sonication of the cells, fractionation on DEAE-Sephadex A-25, urea treatment, and separation on Sephadex G-50. Because M4 was expressed at a low level and eluted differently from DEAE-Sephadex than did the other mutant proteins and together with other proteins (Figure 3), M4 was not pure after the Sephadex G-50 gel filtration. Therefore, an additional preparative agarose electrophoresis step (Johansson, 1972) was added. Pooled protein from fractions 26–50 (10–20 mg of protein in 1 mL of buffer) was used in each run on a 5 × 205 × 110 mm 1% agarose plate (Sea Kem le agarose, FMC Corp.). A paper print of the gel was stained and the M4 protein band cut out and put in a test tube, placed in a freezer for 2–3 h, and then rapidly thawed. The agarose structure was thereby changed, and the protein solution could be separated from the agarose.

The purity of the mutant proteins was checked by both SDS gel and agarose gel electrophoresis in the presence of either

[2] Abbreviations: DEAE, diethylaminoethyl; EDTA, ethylenediaminetetraacetic acid; EMF, electromotive force; NTA, nitrilotriacetate; PIPES, piperazine-*N*,*N*′-bis(2-ethanesulfonic acid); Quin2, 2-[[2-[bis(carboxymethyl)amino]-5-methylphenoxy]methyl]-6-methoxy-8-[bis(carboxymethyl)amino]quinoline; SDS, sodium dodecyl sulfate; Tris, tris(hydroxymethyl)aminomethane.

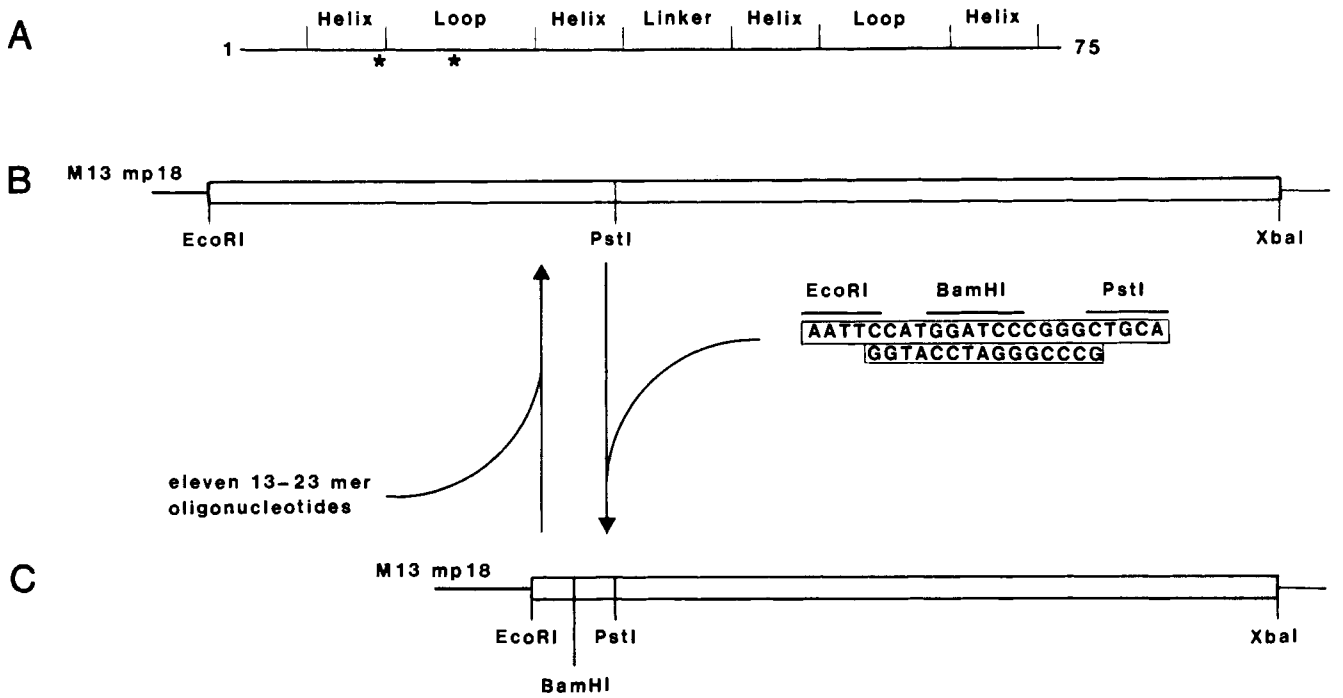

FIGURE 2: Construction of synthetic genes encoding bovine calbindin D_{9k} with amino acid substitutions and deletions. (A) shows the different structural parts of the calbindin molecule. The N-terminal amino acid is marked 1, and the C-terminal amino acid is marked 75. The asterisks show the positions in the protein where amino acid changes were introduced. (B) shows the entire calbindin gene, as previously constructed from oligonucleotides and inserted into bacteriophage M13mp18 (Brodin et al., 1986). The *Eco*RI–*Pst*I DNA segment containing the N-terminal part of the gene was replaced by the shown polylinker sequence to obtain the truncated gene displayed in (C). Full-length calbindin genes with nucleotide substitutions and/or deletions were subsequently assembled by ligation of sets of eleven oligonucleotides, 13–23 nucleotides long, corresponding to both DNA strands, between the *Eco*RI and *Pst*I sites bordering the polylinker.

2 mM EDTA (Figure 4) or 2 mM Ca^{2+} (not shown). The electrophoresis gels show that the proteins are pure and homogeneous. All the proteins have the same mobility on the SDS gel. However, the agarose gel indicates that M4 has less negative surface charge than the others. Amino acid sequencing confirmed that M4 had the intended sequence, and therefore the change in surface charge might be due to an increase in the pK_a of one of the ionizable side chains. Glu-35 is a likely candidate because the loss of the original hydrogen bond to Tyr-13 in an otherwise strongly hydrophobic environment (Szebenyi & Moffat, 1981) would tend to increase the pK_a of this carboxyl group.

Apoproteins (Ca^{2+}-free proteins) were prepared by adjusting aqueous unbuffered solutions of the mutant proteins (1–5 mg/mL) to pH 8 with NH_3 and passing them slowly over a Chelex 100 (Bio-Rad Laboratories) column (1 mL/10 mg of protein) in doubly distilled water adjusted to pH 8 with NH_3. The protein solutions were lyophilized. The residual Ca^{2+} content was determined for each batch of protein by atomic absorption spectroscopy. It was found to vary between 0.01 and 0.1 mol of Ca^{2+}/mol of protein.

Determination of Ca^{2+}-Binding Constants. Two different methods were used in order to cover the whole range of binding constants from 10^4 to 10^9 M^{-1}. All solutions were made in 2 mM Tris-HCl buffer at pH 7.5. The buffer was prepared from doubly distilled water and was stored in a container with a dialysis bag containing Chelex 100. The residual Ca^{2+} in the buffer was always below 1 μM as determined by atomic absorption spectroscopy. Plastic containers and vessels were used throughout except for a thermostated glass cell that was used in the electrode method and quartz cells that were used in the Quin2 method. All chemicals were of the highest quality commercially available. Quin2 (tetrapotassium salt) was from Fluka, Buchs, Switzerland. The porcine calbindin D_{9k} was a gift from Theo Hofmann, Toronto. All pipettes were calibrated by weight to give the correct absolute volumes.

(A) Quin2 Method. Binding constants in the range 10^7–10^9 M^{-1} were obtained from Ca^{2+} titration of the proteins in the presence of the fluorescent Ca^{2+} chelator Quin2 (Bryant, 1985). Quin2 was first dissolved in the buffer to around 27 μM. The Quin2 concentration was determined by measuring the absorbance at 240 nm (ϵ_{240} = 4.2 × 10^4 L·mol^{-1}·cm^{-1}). This value of ϵ was obtained from measurements of the absorbance at 240 nm during a stepwise addition of a Ca^{2+} solution of accurately known concentration to a Quin2 solution beyond saturation. The freeze-dried protein was dissolved in the Quin2 solution to typically 25 μM. The total sample volume was 2.0 mL, and Ca^{2+} solutions ($CaCl_2$ dissolved in the 2 mM Tris-HCl buffer at pH 7.5) were added in 5-μL portions. After each Ca^{2+} addition the solution was mixed well and allowed to equilibrate for 5 min. The Quin2 fluorescence was excited at 339 nm (band-pass 0.5 nm) and measured at 500 nm (band-pass 40 nm), the narrow excitation band-pass being used to minimize the photobleaching of Quin2. The samples were excited just long enough to obtain stable readings (2–5 s).

The two macroscopic binding constants of the protein, K_1 and K_2 (which are sometimes referred to as stoichiometric binding constants and which are defined in Figure 5), were obtained from a least-squares fit to the Quin2 fluorescence intensity as a function of the total calcium concentration. The partitioning of calcium between protein and Quin2, and hence the theoretical fluorescence intensity, was solved iteratively. Equal weight was given to all points in the titration, including the fluorescence intensity before the start of a titration and the intensity after a large final calcium addition. Corrections were made for the initial Ca^{2+} concentration and for the dilutions due to addition of Ca^{2+}. The protein concentration was obtained by weight and was multiplied by a correction factor, which was varied in the minimization procedure. The cor-

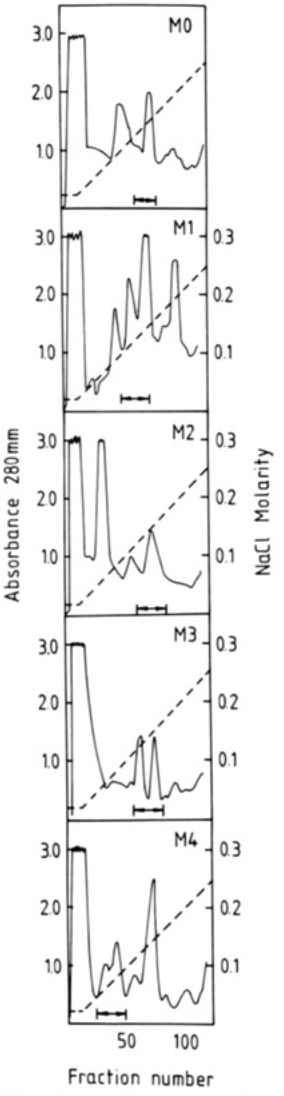

FIGURE 3: Separation of *E. coli* extract using 3 × 20 cm DEAE-Sephadex A-25 columns. The initial buffer was 0.02 M imidazole, 0.02 M NaCl, and 1 mM EDTA at pH 7.0. The proteins were eluted with linear NaCl gradients; 10-mL fractions were collected. The pooled fractions, containing mutant calbindins, are indicated with horizontal arrows.

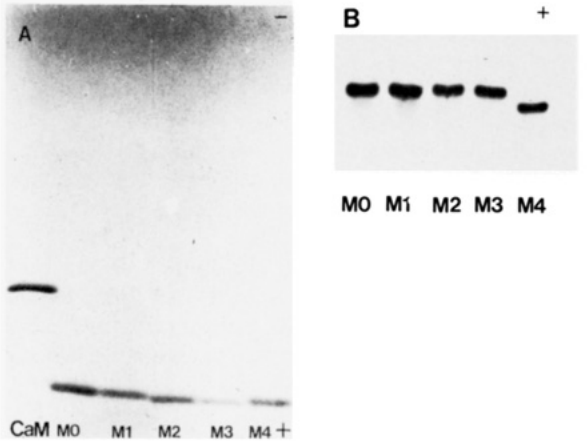

FIGURE 4: Electrophoresis of purified calbindins M0–M4 in (A) SDS–polyacrylamide 10–20% gradient gel and (B) agarose gels run in the presence of 2 mM EDTA.

rection factors converged in all cases to a well-defined value, ranging from 0.5 to 0.9. The correction factors obtained for a specific mutant and batch were highly consistent between different types of experiments—Quin2 method, electrode

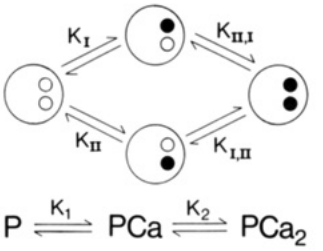

FIGURE 5: Definition of binding constants: macroscopic (or stoichiometric) binding constants, K_1 and K_2, and the microscopic (or site) binding constants, K_I, K_{II}, $K_{I,II}$, and $K_{II,I}$.

method, microcalorimetric measurements, and NMR titrations. There was also good agreement with micro-Kjeldahl analyses on two batches each of M0, M1, and M2.

For M0 and those mutant proteins with two strong Ca^{2+} sites both macroscopic binding constants were allowed to vary during the fitting procedure. For the mutant proteins with the Ca^{2+} affinity of one site well outside the range of the Quin2 method, the second macroscopic binding constant was held fixed at the value obtained from the electrode titrations described below.

The Ca^{2+}-binding constant of Quin2 (tetrapotassium salt) at pH 7.5, K_Q^{Ca}, was determined from a titration of 27 μM Quin2 with Ca^{2+} in the presence of 45 μM EDTA instead of protein. Using 3×10^8 M^{-1} for the Ca^{2+}-binding constant of EDTA at pH 7.5 at zero ionic strength (as an average of published values ranging from 2×10^8 M^{-1} to 4×10^8 M^{-1}), we obtain $K_Q^{Ca} = 1.9 \times 10^8$ M^{-1}, in reasonable agreement with the value obtained by Bryant (1985). The uncertainties in the Ca^{2+}-binding constants reported here do not include uncertainties in K_Q^{Ca}.

The possibility of interactions between Quin2 and calbindin at the concentrations used was ruled out for the case of M0 by using a technique described elsewhere (Chiancone et al., 1986).

(*B*) *Electrode Method.* A Ca^{2+}-selective electrode (Beta Sensor, Lund, Sweden) was used to measure binding constants in the range 10^4–10^7 M^{-1}. To stabilize the electrode and extend the linear region, the Ca^{2+} electrode solution was composed of 10 mM NTA and 11 mM total Ca^{2+} as recently described by Morton et al. (1986). The electrode response to the logarithm of the free calcium concentration was linear between 10^{-8} and 10^{-2} M. Calibrations were performed each day in the range 10^{-6}–10^{-2} M. The slope was maintained over the whole period of use. A few calibrations were carried out in the presence of 75 μM Quin2 to obtain well-defined free calcium concentrations in the range 10^{-9}–10^{-6} M.

The freeze-dried proteins (4.5 mg) were dissolved in the 2 mM Tris-HCl buffer at pH 7.5. The total sample volume was 5.0 mL. Ca^{2+} solutions were added in 50–200-μL portions.

The macroscopic binding constants were obtained from a least-squares fit to the electrode EMF as a function of total calcium concentration. A protein concentration correction factor (cf. above) and an offset parameter corresponding to the offset from the calibration curve intercept were incorporated in the minimization. Both were found to converge to well-defined values. The offset parameter of the best fit agreed well with the offset that was estimated from a large Ca^{2+} addition at the end of each titration. Corrections were made for the initial Ca^{2+} concentrations and for the dilutions due to addition of Ca^{2+}.

Although we could not show directly that calbindin did not interact with the electrode membrane at the concentrations used in our study because of insufficient material, we showed separately that the closely related protein parvalbumin (carp

P5b) did not interfere with the electrode up to a protein concentration of 200 μM as follows. A 1 mM Ca^{2+} buffer was prepared in 2 mM Tris-HCl buffer at pH 7.5. Parvalbumin was dissolved in the Ca^{2+} buffer and was dialyzed against the same Ca^{2+} buffer to obtain the same free Ca^{2+} concentration in both solutions. The Ca^{2+} electrode was placed in 5 mL of the Ca^{2+} buffer used to dialyze the parvalbumin. When a stable reading was obtained, the protein solution was added in steps to give 10 or 20 μM, up to a total protein concentration of 200 μM. The electrode EMF was not affected by the addition of parvalbumin. Calbindin was assumed to behave in the same way.

(*C*) $\Delta\Delta G$. The calculated free energy of interaction between the two sites, $\Delta\Delta G$ (Weber, 1975), depends on the ratio of the two macroscopic binding constants, K_1 and K_2, and the ratio, η, of the two site binding constants to the individual sites in the apoprotein, K_I and K_{II} (Figure 5). $\Delta\Delta G$ is related to the ratio of the site binding constants of one site in the presence ($K_{I,II}$) and absence (K_I) of Ca^{2+} in the other site:

$$\Delta\Delta G = -RT \ln (K_{I,II}/K_I) = -RT \ln (K_{II,I}/K_{II})$$

Using the relations between macroscopic and microscopic binding constants

$$K_1 = K_I + K_{II}$$

$$K_2 = K_I K_{II,I}/(K_I + K_{II})$$

one can express $\Delta\Delta G$ as a function of K_1, K_2, and the ratio of K_{II} to K_I:

$$\Delta\Delta G = -RT \ln \left(\frac{K_2}{K_1} \frac{(\eta + 1)^2}{\eta} \right)$$

where $\eta = K_{II}/K_I$.

Thus, knowledge of K_1, K_2, and η yields $\Delta\Delta G$ and also the four site binding constants. η cannot be deduced from the Quin2 or electrode measurements and must be determined separately by a method that distinguishes between Ca^{2+} binding to the two sites of the protein (e.g., NMR). Since the function $(1 + \eta)^2/\eta$ has a minimum at $\eta = 1$, a lower limit of the absolute value of $\Delta\Delta G$ can be obtained from K_1 and K_2 by assuming that both sites in the protein are equal ($K_I = K_{II}$).

NMR Studies. (*A*) *Sample Preparation.* For all NMR studies the freeze-dried apoproteins were dissolved in D_2O to a concentration of 1 mM. The pH was adjusted to 8.0 for the ^1H and ^{43}Ca NMR studies and to 6.5 for the ^{113}Cd NMR studies. The metal ion titrations were performed by adding small portions of 25 mM solutions of the metal ion. After each addition the pH was adjusted back to its original value by adding either DCl or NaOD.

For the metal NMR studies samples enriched in either ^{43}Ca (50%, Technab Export, Moscow) or ^{113}Cd (95%, Oak Ridge, TN) were used.

(*B*) *Spectra.* ^1H NMR spectra were obtained on a Nicolet 360 WB spectrometer at 361.79 MHz with 5-mm NMR tubes. To minimize the signal from residual HDO, the water resonance was first inverted with a selective, low-power pulse, and when the water magnetization had relaxed back to zero, a nonselective 90° pulse was applied.

^{43}Ca NMR spectra were obtained on the Nicolet 360 WB spectrometer at 24.34 MHz. A homemade horizontal probe with a solenoidal coil was used (Drakenberg et al., 1983). To minimize the effects from acoustic ringing, the RIDE sequence was used, with a 90° pulse length of 40 μs (P. D. Ellis, personal communication; Belton, 1985). One thousand data points were recorded for a spectral width of ±10 000 Hz. Up to 5×10^6 transients were accumulated during a total time of 15 h. The transients were added together in blocks of 10^4, which were then stored on a disk in double precision.

^{113}Cd NMR spectra were obtained on a homemade spectrometer, using an Oxford Instruments 6T magnet, at 56.55 MHz with the same type of probe as for ^{43}Ca NMR. The normal one-pulse experiment was used, and 25 000–50 000 transients were accumulated, with a pulse length of 10 μs (45°). The pulse repetition time was 0.6 s.

(*C*) *Determination of Ca^{2+} Exchange Rates.* The shape of the ^{43}Ca NMR signal will depend on the off-rate of the Ca^{2+} ion from its binding site in the protein when the off-rate is in the intermediate range (10^1–10^4 s^{-1}). To obtain the exchange rate at 25 °C, k_{off}^{25}, and the quadrupole coupling constant, χ, the experimental and calculated temperature dependences have been compared. The theoretical temperature dependence was calculated as outlined in detail by Tsai et al. (1987). While the $\Delta H^{\ddagger}$ and $\Delta S^{\ddagger}$ values are uncertain, the $\Delta G^{\ddagger}$ at 25 °C and therefore also k_{off}^{25} are obtained with high accuracy.

(*D*) *Denaturation Studies.* ^1H NMR spectra were recorded for samples containing 1 mM apoprotein at pH 7.5. Spectra were obtained at 5-deg intervals from 25 to 70 °C.

Microcalorimetry. All the microcalorimetric measurements were made at 25 °C by using an LKB batch microcalorimeter equipped with an LKB titration syringe assembly mounted on the outside of the calorimeter block (Chen & Wadsö, 1982). The differential calorimetric signal was amplified by a Keithley 148 nanovoltmeter. The output voltage–time curve was integrated (20 min) by a microprocessor which also controlled the injections from the syringes into the cells and the rotation of the calorimeter block in connection with each injection. The calorimeter was calibrated electrically and also by using the standard procedure of protonation of Tris with HCl (Öjelund & Wadsö, 1968).

All measurements were made in 20 mM PIPES buffer at pH 7.0. The protein concentration in the reaction cell (4–5 mL) was 0.2–0.8 mg/mL. The Ca^{2+} concentration of the titrating solution ($CaCl_2$ dissolved in the PIPES buffer) ranged from 10 to 90 mM, depending of the heat effects to be measured, the binding constants, and the protein concentration. Injection of Ca^{2+} solution to the reaction cell was always accompanied by an equally large injection (5–15 μL) to the reference cell containing only the buffer, thereby eliminating the need for separate dilution experiments.

The calorimetric titration curves were analyzed by using a modified version of a computer program specially written for ligand binding experiments (Karlsson & Kullberg, 1976). The program does not allow the simultaneous determination of equilibrium constants and enthalpy changes if the value of the highest constant exceeds 10^6 M^{-1}, but it can be used for calculations of ΔH values if fixed values of the binding constants, determined by other methods, are used.

Results

Ca^{2+}-Binding Constants. The macroscopic binding constants, K_1 and K_2, and their uncertainties are summarized in Table I. The reproducibility of the binding constant measurements was generally very good, and the theoretical titration curves show an excellent fit to the experimental data, as exemplified in the case of the Quin2 method in Figure 6A and of the electrode measurements in Figure 6B. The precision of the results is very high in the range 10^8–10^9 M^{-1}, i.e., when the affinity of the protein is similar to that of Quin2 (1.9×10^8 M^{-1}), due to the fact that the method involves measurement of the distribution of calcium between Quin2 and the

Table I: Macroscopic Ca^{2+}-Binding Constants of Calbindins at 25 °C

protein	K_1 (M^{-1})[a]	K_2 (M^{-1})[a]
M0	(2.2 ± 0.3) × 10^8 [8][b]	(3.7 ± 0.4) × 10^8 [8][b]
M1	(6.5 ± 1.5) × 10^7 [6][b]	(8 ± 6) × 10^6 [8][b,c]
M2	(1.7 ± 0.2) × 10^8 [5][b]	(5 ± 2) × 10^5 [1][c]
M3	(8.0 ± 1.5) × 10^7 [7][b]	(5 ± 2) × 10^5 [1][c]
M4	(3.7 ± 0.5) × 10^8 [5][b]	(2.5 ± 0.4) × 10^8 [5][b]
porcine	(8.0 ± 1.5) × 10^7 [4][b]	(1.8 ± 0.2) × 10^8 [4][b]

[a] The number in brackets is the number of measurements. The uncertainties are the standard deviations in these measurements and do not include uncertainties in K_Q^{Ca}. The uncertainties in K_2 of M2 and M3 are estimates.

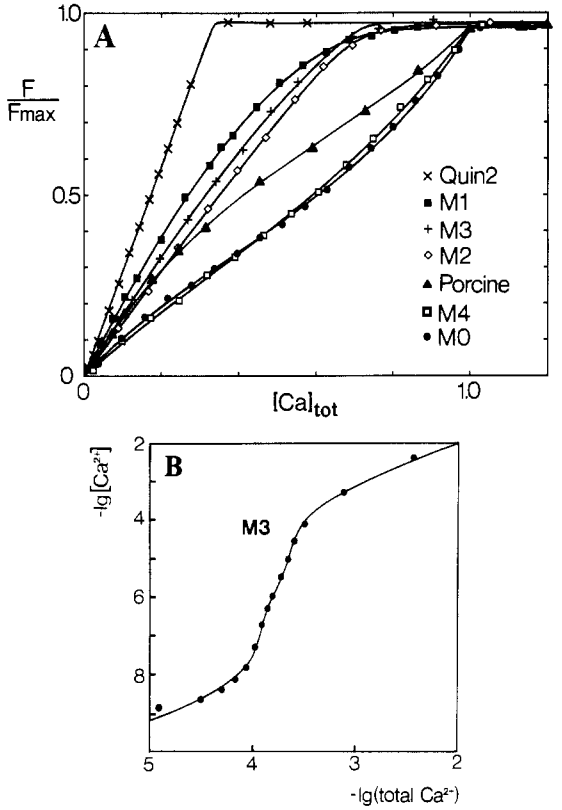

FIGURE 6: (A) Titrations of Quin2 with Ca^{2+} in the presence and absence of calbindins. The Quin2 fluorescence intensity is plotted versus total Ca^{2+} concentration. $[Ca^{2+}]_{tot}$ = 1 corresponds to 3-$[Quin2]_{tot}$ or $[Quin2]_{tot}$ + 2$[protein]_{tot}$ for titrations in the absence and presence of protein, respectively. The concentrations of Quin2 and protein for the data sets are given below. The values of K_1 and K_2 for the fitted curves are given in parentheses. For M2 and M3 K_2 is the value obtained by the electrode method. These constants differ slightly from those given in Table I because the constants in the Table I are averages of several titrations. Concentrations are as follows: (×) 27.0 μM Quin2; (■) 29.0 μM Quin2, 24.2 μM M1 (K_1 = 6.5 × 10^7 M^{-1}, K_2 = 1 × 10^7 M^{-1}); (+) 27.1 μM Quin2, 17.0 μM M3 (K_1 = 8.5 × 10^7 M^{-1}, K_2 = 5 × 10^5 M^{-1}); (◇) 31.1 μM Quin2, 23.1 μM M2 (K_1 = 1.7 × 10^8 M^{-1}, K_2 = 5 × 10^5 M^{-1}); (▲) 27.0 μM Quin2, 26.6 μM porcine calbindin (K_1 = 8.0 × 10^7 M^{-1}, K_2 = 1.8 × 10^8 M^{-1}); (●) 27.4 μM Quin2, 27.5 μM M0 (K_1 = 2.3 × 10^8 M^{-1}, K_2 = 3.6 × 10^8 M^{-1}); (□) 26.1 μM Quin2, 26.6 μM M4 (K_1 = 3.6 × 10^8 M^{-1}, K_2 = 2.4 × 10^8 M^{-1}). (B) Titration of 120 μM M3 with Ca^{2+} using the Ca^{2+}-selective electrode. The plotted curve was obtained from a least-squares fit to the data and corresponds to K_1 = 6 × 10^7 M^{-1} and K_2 = 4.8 × 10^5 M^{-1}.

protein. The major sources of error are the photobleaching of Quin2 and the slow equilibration after addition of calcium. Although an error in K_Q^{Ca} would affect the absolute values of the binding constants, it does not affect the comparative values of the different proteins.

The electrode method gives slightly larger uncertainties than the Quin2 method due to the fact that the measured quantity

Table II: Thermodynamic Quantities for Binding of Ca^{2+} to Wild-Type Calbindin and Mutant Proteins at 25 °C

protein	site	$\Delta G°$ (kJ·mol^{-1})[a]	$\Delta H°$ (kJ·mol^{-1})[b]	$\Delta S°$ (J·K^{-1}·mol^{-1})
M0	I	−48	−8 ± 1	134
	II	−48	−8 ± 1	134
M1	I	−40	−11 ± 1	97
	II	−45	−13 ± 1	107
M2	I	−33	+5 ± 2	128
	II	−47	−8 ± 1	131
M3	I	−33	+5 ± 2	128
	II	−45	−7 ± 1	128
M4	I	−48	−8 ± 1	134
	II	−48	−8 ± 1	134

[a] Calculated from the binding constants in Table I. [b] The uncertainties given are the overall errors, including estimated uncertainties in the protein concentration.

Table III: ^{43}Ca and ^{113}Cd Chemical Shifts (δ), Quadrupole Coupling Constants, and Dissociation Rate Constants for Metal Ion Bound to Calbindin and Mutants[a]

		^{43}Ca			^{113}Cd δ (ppm)	
protein	site	k_{off} (s^{-1})	δ (ppm)	χ (MHz)	Cd_1[b]	Cd_2[c]
M0	I	~3	−9	1.4		−156
	II	~3	7	1.0	−105	−110
M1	I	430 ± 100		1.4		−88
	II	<10	7	1.0	−109	−110
M2	I	5000 ± 1000		1.0		
	II	<10	8	1.0	−112	−115
M3	I	5000 ± 1000		1.0		
	II	<10	8	1.0	−113	−115
M4	I	~3	−9	1.4		−155
	II	~3	7	1.0	−105	−110

[a] All values refer to 25 °C. [b] Below Cd_1 are listed ^{113}Cd chemical shifts for a protein with one bound Cd^{2+} ion. [c] Below Cd_2 are listed ^{113}Cd chemical shifts for a protein with two bound Cd^{2+} ions.

(the electrode EMF) does in this case depend on the free calcium concentration, which for the observed binding constants and protein concentrations used is only a very small fraction of the total added calcium. The relatively large uncertainty of K_2 in the case of M1 is due to the fact that this constant falls outside the optimal range of both methods.

The data summarized in Table I differ somewhat from those given earlier in a preliminary report (Forsén et al., 1987) because at that stage the binding affinities were analyzed in terms of two noninteracting sites. Furthermore, we have since succeeded in extending the linear region of the calcium-selective electrode into the relevant range 10^{-8}–10^{-5} M.

Microcalorimetry. The results of the thermodynamic measurements of Ca^{2+} binding to the wild-type calbindin and the mutants are summarized in Table II. The $\Delta G°$ values for M0 and M4 were calculated by using average values of the binding constants. For these two proteins the assignment of the $\Delta H°$ values to the individual sites was arbitrary; the total enthalpy change for the binding of two Ca^{2+} was in both cases −16 kJ·mol^{-1}. The enthalpy changes for the other proteins and the individual site values were calculated by using the computer program of Karlsson and Kullberg (1976) by fixing the binding constants as given in Table I and finding the best-fit values of $\Delta H°$ in the usual way.

Cadmium-113 NMR. The results are summarized in Table III. Spectral shifts are reported relative to 0.1 M $^{113}CdClO_4$ at pH 7. Titrations of the wild-type and four mutant calbindins with $^{113}Cd^{2+}$ always result first in the appearance of a ^{113}Cd resonance at −105 to −113 ppm. The intensity of this signal increases linearly up to a $[Cd^{2+}]/[protein]$ ratio of 1.

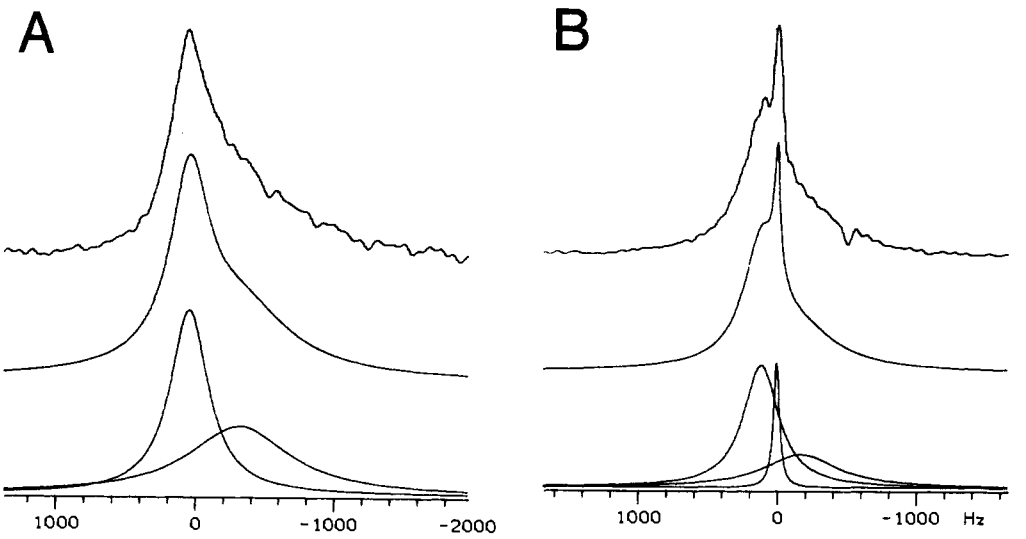

FIGURE 7: ^{43}Ca NMR spectra at 24.34 MHz from a solution with 1 mM calbindin (M4) at pH 8.0. Top, experimental spectrum; middle, calculated spectrum; bottom, individual Lorentzian lines. (A) $[Ca^{2+}]/[M4] = 0.8$. The observed band can be resolved into two Lorentzian signals with approximately equal integrated intensity. One of the signals has a chemical shift, line width, and quadrupole coupling constant typical for EF-hand calcium sites, $\delta = 7$ ppm, $\Delta\nu = 350$ Hz, and $\chi = 1.0$ MHz, whereas the other line is broader ($\Delta\nu_{1/2} = 600$–800 Hz, $\chi = 1.4$ MHz) and is shifted upfield to −9 ppm. (B) $[Ca^{2+}]/[M4] = 2.2$.

At higher cadmium concentrations this resonance is displaced toward lower frequency, maximum displacement 5 ppm, as a result of Cd^{2+} entering also into site I.

For M0 and M4 there is, in addition to the change in the chemical shift, also a broadening of the resonance for samples with $[Cd^{2+}]/[protein]$ ratios between 1 and 2. For ratios exceeding 2 the resonance has moved to −110 ppm and become sharp. When the spectra are recorded at 5 °C (instead of 25 °C), a second broad resonance is observed at ca. −150 ppm.

For M1 the first resonance to appear is only displaced from −109 to −110 ppm with no observable broadening as more than 1 equiv[3] of Cd^{2+} is added. At a $[Cd^{2+}]/[M1]$ ratio of 2 a second broad resonance with a chemical shift of −88 ppm appears.

For M2 and M3, addition of up to 1 equiv of Cd^{2+} results in a ^{113}Cd NMR signal at −112 and −113 ppm, respectively, both of which move to −115 ppm upon further addition of Cd^{2+}. These resonances have the same line width throughout the titration, and no further signals can be observed for protein-bound Cd^{2+}.

Calcium-43 NMR. The results are summarized in Table III. ^{43}Ca NMR spectra of M0 and M4 containing less than 2 equiv of Ca^{2+} invariably contain two broad overlapping resonances, exemplified in Figure 7A. When more than 2 equiv of Ca^{2+} is present, a third sharp resonance is observed with a shift close to that of free calcium ions (Figure 7B).

A sample with a $[Ca^{2+}]/[M4]$ ratio of 2.5 was used to study the temperature dependence of the ^{43}Ca NMR signals between 25 and 55 °C. The widths of the two broad lines, originating from Ca^{2+} ions bound to the two sites in the protein, at 55 °C, are reduced to less than half of their widths at 25 °C, whereas the sharp line is unaffected up to 45 °C and shows a minor broadening at 55 °C (Figure 8). The calcium off-rate from the binding sites in M4 is thus too slow to be measured accurately with ^{43}Ca NMR but can be estimated to be around 3 s^{-1} at 25 °C for both sites. Exactly the same is found for M0.

Addition of 0.5 mM Ca^{2+} to a 1 mM solution of M1 results in a 350-Hz broad ^{43}Ca resonance with a chemical shift of 7 ppm. Upon further addition of calcium, to almost 2 mM Ca^{2+},

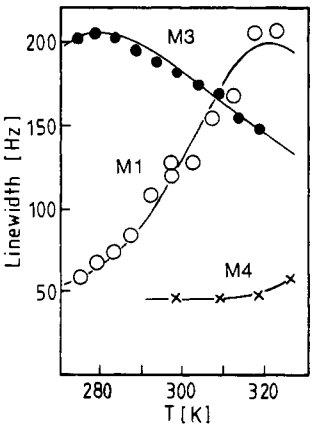

FIGURE 8: Temperature dependence of the line width of the ^{43}Ca NMR signal from three of the mutant calbindins. The curves are calculated on the basis of the assumption that there is exchange between free Ca^{2+} ions and ions bound to one of the sites in the protein.

the resonance broadens slightly, to 400 Hz, and is displaced upfield to 5 ppm. At Ca^{2+} concentrations above 2 mM the ^{43}Ca resonance becomes sharper and moves further upfield. At $[Ca^{2+}] = 3$ mM the observed resonance has moved to 0 ppm and the width has been reduced to $^1/_3$ of its maximum value. During this titration the shape of the NMR signal does not deviate appreciably from that of a Lorentzian line. The temperature dependence of the ^{43}Ca NMR signal from a sample containing 1 mM M1 and 3 mM Ca^{2+} is shown in Figure 8. By use of total band shape analysis (Drakenberg et al., 1983) the experimental temperature dependence can be fitted with $\Delta H^{\ddagger} = 49.0$ kJ·mol^{-1} and $\Delta S^{\ddagger} = -30$ J·K^{-1}·mol^{-1}, giving $k_{off} = 430 \pm 100$ s^{-1} at 25 °C. This band shape analysis also resulted in $\chi = 1.4$ MHz.

The addition of up to 1 mM Ca^{2+} to a 1 mM solution of M2 or M3 results in a 350-Hz broad ^{43}Ca resonance with a chemical shift of 8 ppm. Increasing the Ca^{2+} concentration above 2 mM results in reduction of the ^{43}Ca line width, without any noticeable deviation from a Lorentzian line shape. Figure 8 shows the temperature dependence of the line width of the ^{43}Ca signal for a sample containing 1 mM M2 and 3 mM Ca^{2+}. As for the other mutant proteins, total band shape analysis was used to find kinetic parameters. These calculations resulted in $\Delta H^{\ddagger} = 34.1$ kJ·mol^{-1} and $\Delta S^{\ddagger} = -60$ J·

[3] One equivalent = 1 mol of Ca^{2+}/mol of protein.

Table IV: ^{1}H Chemical Shifts[a] for Some Selected Aromatic Resonances from Apo as well as Calcium-Saturated Forms of M0 to M4

protein	Tyr-13 2,6H	Tyr-13 3,5H	Phe-10 4H	Phe-10 4H	Phe 4H	Phe-66 2,6H	Phe-63 2,6H	Phe-10 2,6H
M0 (apo)	7.73	6.77					6.83	6.57
M1 (apo)	7.62	6.78					6.78	6.61
M2 (apo)	7.54	6.77					6.82	6.66
M3 (apo)	7.55	6.78					6.78	6.66
M4 (apo)							6.82	6.60
M0·Ca_2	7.52	6.83	7.69	7.42	7.09	7.00	6.57	6.39
M1·Ca_2	7.52	6.82	7.68	7.42	7.08	7.00	6.57	6.39
M2·Ca_2	7.53	6.81	7.64	7.41	7.09	7.05	6.71	6.51
M3·Ca_2	7.55	6.82	7.65	7.43	7.08	7.05	6.71	6.50
M4·Ca_2			7.72		7.10	6.99	6.57	6.41

[a] The assignments for the M0 resonances are those proposed by Dalgarno et al. (1983), and the assignments for the mutant proteins have been made in analogy with these.

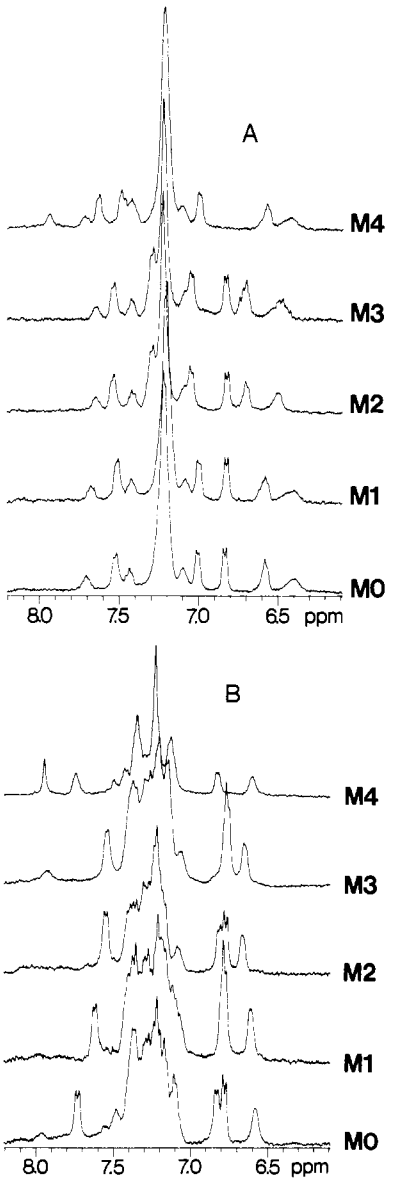

FIGURE 9: 360-MHz ^{1}H NMR spectra of the aromatic region of the five proteins M0 to M4. The signal at 8 ppm is from a slowly exchanging NH proton. (A) Ca^{2+}-loaded forms; (B) apoproteins.

K^{-1}·mol^{-1} for both M2 and M3, which gives k_{off} = 5000 ± 1000 s^{-1} at 25 °C and χ = 1.0 MHz for both M2 and M3.

Proton NMR. The aromatic regions of the ^{1}H NMR spectra of M0 through M4 in the absence and presence of Ca^{2+} are shown in Figure 9. The proton NMR spectra of the Ca^{2+}-loaded as well as the apo forms of the four mutant proteins are very similar to those of the wild-type protein, with the exception of the replacement of the Tyr signals with Phe signals in M4. Table IV lists the chemical shifts of some resonances that have been tentatively assigned to specific amino acids in bovine calbindin (Dalgarno et al., 1983).

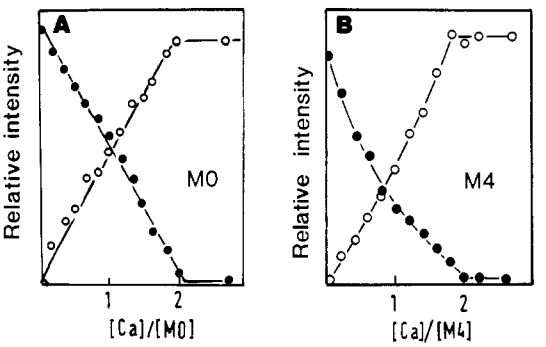

FIGURE 10: Intensities of selected ^{1}H NMR signals of M0 and M4 as a function of Ca^{2+} to protein ratios. Protein concentration 1 mM and pH 8.0. (A) M0: (○) Phe-66 resonance at 6.98 ppm; (●) Tyr-13 resonance at 6.77 ppm. (B) M4: (○) Phe-66 resonance at 6.98 ppm; (●) Phe-63 resonance at 6.82 ppm.

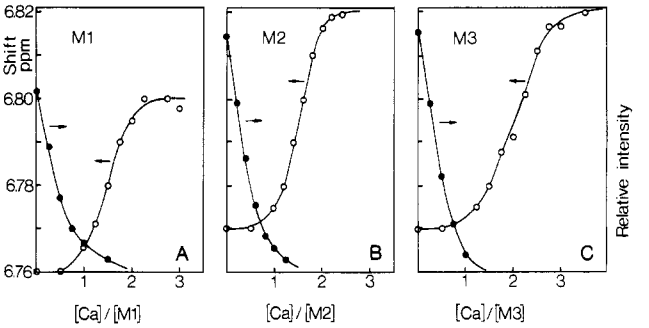

FIGURE 11: Intensity and chemical shift changes of selected ^{1}H NMR signals of M1–M3 as a function of Ca^{2+} to protein ratios. Protein concentration 1 mM and pH 8.0. (●) Intensity change of the resonance Phe (Phe-10 2,4H) with a chemical shift of 6.61–6.66 ppm; (○) shift change in the Tyr-13 3,5H resonance. (A) M1; (B) M2; (C) M3.

Despite these similarities there are distinct differences between the spectra during the calcium titrations. For M0 and M4 the Ca^{2+} ion exchange rates are slow on the NMR time scale and two overlapping spectra are seen during the titration, one from the apoprotein and one from the calcium-saturated protein, with no clear indication of a protein with only *one* bound Ca^{2+} ion. Several signals decrease or increase with added Ca^{2+} for $[Ca^{2+}]/[protein]$ ratios up to 2. This is exemplified for a few resonances from M0 and M4 in Figure 10.

For M1, M2, and M3, addition of small amounts of Ca^{2+}, <1 equiv, results in decreasing intensities of some resonances and the appearance of new lines, as expected when the first bound Ca^{2+} ion is in slow exchange with the bulk solution.

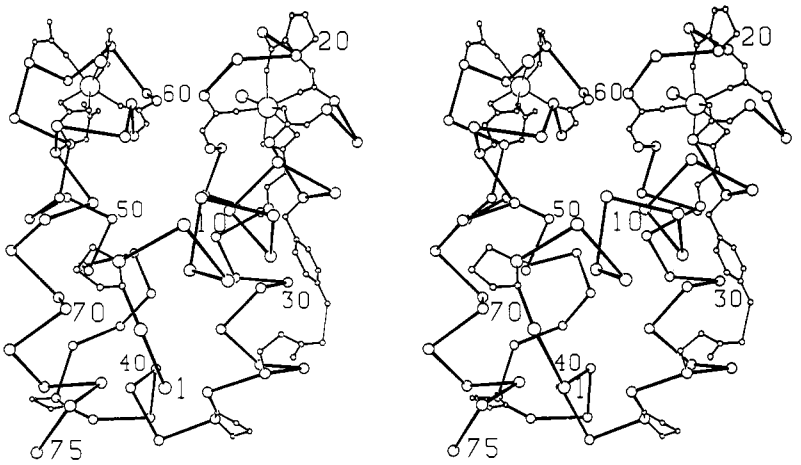

FIGURE 12: Stereoview of the α-carbon structure of bovine calbindin D_{9k} according to crystallographic analysis (Szebenyi & Moffat, 1986). Calcium ligands and Tyr-13 and Glu-35 side chains are included. Figure kindly provided by Dr. D. Szebenyi, Cornell University.

When more than 1 equiv of Ca^{2+} is added, however, the shifts of some lines are gradually changed as expected when the calcium ions causing this change are in fast exchange. Some resonances in M1 also become broadened during the titration, showing that the ion exchange is not sufficiently fast to completely average out the effect due to shift differences between M1·Ca and M1·Ca_2. Panels A, B, and C of Figure 11 show examples of the changes in intensities and shifts for some of the resonances from M1, M2, and M3, respectively.

In the shift range 5.1–5.6 ppm of the ^1H NMR spectrum of M0—a region usually attributed to α-protons in β-sheet structures—a well-resolved signal is observed at low field (5.51 ppm). This resonance is also present in the ^1H NMR spectra of M1 and M4, but not in those of M2 and M3, and has been assigned to one of the α-protons of Gly-18 in the wild-type protein by Dalgarno et al. (1983). Recent two-dimensional ^1H NMR studies at 500 MHz have however shown that this assignment is incorrect (W. Chazin, personal communication), but at the time of writing the true identity of this signal has not been established.

The temperature variation in the chemical shifts was followed for the phenylalanine resonance at highest field in apo-M0 and apo-M4 as well as for the α-proton resonance at lowest field in apo-M4. Only very small temperature effects were observed in the ^1H NMR spectrum of apo-M0 up to a temperature of 70 °C. For apo-M4, on the other hand, there are noticeable effects on the aromatic resonances above 50 °C, whereas the low-field α-proton resonances remain unaffected by temperatures up to 70 °C.

Discussion

Before we discuss the biophysical measurements on the five different calbindins studied in this work, it is necessary to outline the structural features of the protein. A detailed description of the X-ray structure refined to a resolution of 2.3 Å of the minor A form of bovine calbindin D_{9k} was recently given by Szebenyi and Moffat (1986). The protein, which is approximately spherical (20 × 20 × 30 Å), has four main α-helices and two Ca^{2+}-binding loops (Figure 12). The helices, in this work designated A–D, comprise amino acid residues 3–14, 24–36, 45–54, and 62–75, respectively. One of the two Ca^{2+}-binding loops occurs between helices A and B (site I) and the other between helices C and D (site II). An approximate 2-fold axis relates the two Ca^{2+}-binding domains. Three reverse turns are observed: at residues 17–20 (Pro at the fourth position), 19–22 (Pro at the second position), and 42–45 (Pro at the second position).

The "interior" of the molecule shows a loose clustering of several hydrophobic side chains; in particular, three phenylalanine rings come very close in space: Phe-10, Phe-63, and Phe-66. The Ca^{2+}-binding loops appear to constitute the least mobile parts of the molecule—the temperature *B* factors have pronounced minima in these regions with the lowest overall *B* factors observed in the loop constituting Ca^{2+} site II.

Both Ca^{2+} ions are roughly octahedrally coordinated with protein oxygen atoms at the x, y, z, and $-y$ vertices, a bidentate carboxyl group at $-z$, and a water molecule at $-x$. There are also, however, some striking differences between the structure of the two sites. Whereas the C-terminal site (II) has a general structure very similar to the archetypal EF-hand site as observed in parvalbumin (Kretsinger & Nockolds, 1973; Moews & Kretsinger, 1975), troponin C (Herzberg & James, 1985a,b; Sundralingam et al., 1985), and calmodulin (Babu et al., 1985, Kretsinger & Weissman, 1986), the existence of an extra residue between vertices x and y and between z and $-y$ in site I makes the fold in the N-terminal half of this loop different from that in site II. As a consequence the oxygen ligands in site I are predominantly backbone carbonyls with only one negatively charged carboxylate group. By contrast, three carboxylates are Ca^{2+} ligands in site II. Despite this marked difference in charge and peptide fold the Ca^{2+} affinities of both sites are remarkably similar as will be discussed in some detail below. Another consequence of the differences between the structures of sites I and II according to Szebenyi and Moffat (1983) is that removal of Ca^{2+} from site I cannot occur without significant rearrangement of the loop with a likely influence on the loop of site II. Of considerable interest with regard to the site–site interaction and cooperative Ca^{2+} binding in calbindins D_{9k} is a pair of hydrogen bonds between amino acids Leu-23 and Val-61 that each form part of two short antiparallel β-sheet strands. Another nonhelix hydrogen bond, between the side chains of Tyr-13 and Glu-35, links helix A with helix B (cf. Figure 1 and Figure 12). Otherwise, interdomain helix–helix contacts are exclusively hydrophobic.

Structural Aspects. Although detailed structural studies on the mutant calbindins have still to be carried out, it appears obvious from the observed ^1H NMR spectra that no major changes in overall tertiary structure have been caused by the modifications and/or deletions. The spectral similarities between the wild-type and mutant proteins are particularly striking for the proteins in the Ca^{2+}-loaded forms. This result is perhaps not surprising in view of the extraordinary thermal stability of mammalian calbindins—they can be treated for several minutes in boiling water without being irreversibly

denatured. Computer modeling experiments[4] on M1, M2, and M3 indicate that the change Pro-20 → Gly in M1 can easily be accommodated within the same structural framework as M0. As expected, the deletions in M2 and M3 required considerable restructuring of the whole Ca^{2+}-binding loop of site I in the modeling experiments. That the change from Tyr-13 to Phe in M4 imposes no changes in this Ca^{2+}-binding loop is hardly surprising.

Qualitative structural information on the mutant calbindins is also available through the ^{113}Cd NMR data. The Cd^{2+} ion has an ionic radius very similar to that of the Ca^{2+} ion, and a large body of spectroscopic and biochemical evidence on EF-hand type Ca^{2+}-binding proteins has shown that the Cd^{2+} ion is an excellent substitution probe for the Ca^{2+} ion (Vogel & Forsén, 1987). In an earlier study we have also demonstrated that addition of Cd^{2+} and Ca^{2+}, respectively, to the metal ion free form of porcine calbindin D_{9k} induces similar if not identical conformational changes (Vogel et al., 1985) but that the binding of Cd^{2+} to the protein is sequential, site II being filled first. This fact allowed us also to identify certain resonances in the ^1H NMR spectra that are primarily affected by the binding of the first or second Cd^{2+} ion. Some ^1H NMR signals in bovine calbindin show the same behavior—a result that we have exploited in assessing the relative magnitudes of the site binding constants in M0 and M4 as discussed further below.

As can be seen in Table III, the chemical shift of the ^{113}Cd NMR signal associated with site II is typical of that of other EF-hand sites (δ = −88 to −120 ppm). The chemical shift of the $^{113}Cd^{2+}$ ion in site I (−156 ppm in M0) is quite extreme, and only one ^{113}Cd NMR signal occurring at higher field has been reported [horseradish peroxidase (Morishima et al., 1986)]. In addition, a site–site interaction between sites I and II is manifested in a displacement of the ^{113}Cd NMR signal of site II when a second Cd^{2+} ion is entering into site I. We will in the following denote this type of displacement $\Delta\delta_{II,I}$.

It may be inferred from the near constancy of the chemical shifts of the $^{113}Cd^{2+}$ ion in site II in the wild-type and mutant proteins (cf. Table III) that the structure of the ligand sphere in this site is only slightly perturbed by the modification at site I. Although the deviations from the wild-type values are most marked in M2 and M3, the differences with respect to M0 (ca. 8 ppm) are small compared to the total range of chemical shifts observed for EF-hand sites (about 30 ppm). By contrast, the substitution Pro-20 → Gly (M1) has a pronounced effect on the ^{113}Cd shift in site I—a change by nearly 70 ppm. Since the modifications at site I in M2 and M3 also have the effect of lowering the binding constant of Ca^{2+} and Cd^{2+} (cf. below), we are unable to determine the ^{113}Cd chemical shifts in these proteins. The modification Tyr-13 → Phe (M4) has no measurable effects on the ^{113}Cd NMR chemical shifts from either of the two cation-binding sites—the hydrogen bond Tyr-13–Glu-35 clearly plays no crucial role in maintaining the fold in the Ca^{2+}-binding loops.

The displacement $\Delta\delta_{II,I}$, of the ^{113}Cd NMR signal of site II as site I is being filled, reflects the concomitant structural changes in site II. The value of $\Delta\delta_{II,I}$ = 5 ppm observed in M0 is close to the shift displacement observed in porcine calbindin D_{9k} when a Ca^{2+} ion rather than a Cd^{2+} ion is entering into site I (Vogel et al., 1985). This indicates that the structural changes induced by Cd^{2+} and Ca^{2+} are very similar. Interestingly, the values of $\Delta\delta_{II,I}$ observed in M1, M2, and M3 have the same sign but are smaller than in M0 and M4. According to the X-ray diffraction studies, Ca^{2+} site I in the wild-type calbindin is very rigid with an inferred limited ability to adjust to different-sized cations. It seems plausible that a change such as Pro-20 → Gly would make this site more flexible and that conformational changes accompanying cation binding would be more easily accommodated. It is presently difficult to predict what effect a deletion of a whole amino acid in the site would have on the structural changes accompanying the binding process since a considerable restructuring of the loop must have occurred.

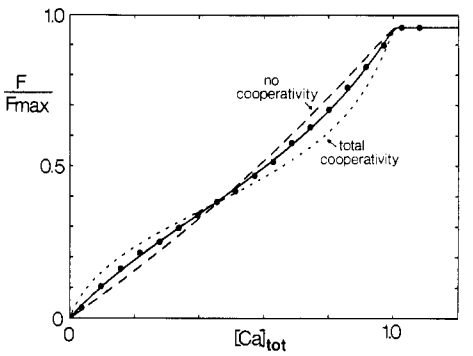

FIGURE 13: Titration of 27.4 μM Quin2 with Ca^{2+} in the presence of 27.5 μM M0. The Quin2 fluorescence intensity is plotted versus total Ca^{2+} concentration. $[Ca^{2+}]_{tot}$ = 1 corresponds to $[Quin2]_{tot}$ + $2[M0]_{tot}$. (●) Experimental data points. (– –) Best fit to a model with two noninteracting sites. (—) Best fit to a model that allows for site–site interaction. (- - -) Calculated curve for the case of very strong site–site interaction ($K_1 = 2.2 \times 10^6$ M^{-1}, $K_2 = 3.7 \times 10^{10}$ M^{-1}).

Equilibrium and Kinetic Properties. The Quin2 titrations convincingly show that M0 binds two Ca^{2+} ions cooperatively and with high affinity ($K_1 = 2.2 \times 10^8$ M^{-1}, $K_2 = 3.7 \times 10^8$ M^{-1}). In the Quin2 fluorescence curve the cooperativity is manifested as a slight S shape, which cannot be reproduced by a model that assumes two noninteracting binding sites. A model that allows for interaction between the sites is, however, capable of fitting smoothly to the Quin2 fluorescence data. Figure 13 shows the data from a single titration of M0 in the presence of Quin2 together with the curves of best fit to models with and without site–site interaction, plus a curve for total cooperativity. Since the Quin2 fluorescence intensity does not distinguish between binding to the two sites of the protein, we can obtain only macroscopic binding constants and not binding constants of the individual sites. There is an infinite number of combinations of the site binding constants (Figure 5) that all yield the same values of K_1 and K_2 and hence exactly the same appearance of the Quin2 fluorescence curve (Klotz & Hunston, 1979).

To proceed from the determined values of K_1 and K_2 to the free energy of interaction between the sites, $\Delta\Delta G$, we need additional information, for example, the ratio, η, of the two site binding constants, K_I and K_{II}. To determine η we need to monitor the distribution of bound Ca^{2+} between the two sites during a titration. This can, in the case of slow exchange, be done by following the intensity of an NMR signal that is affected only by calcium binding to one of the two sites, while the binding of calcium to the other site leaves this signal unaffected. The intensity of such a signal will change linearly with the concentration ratio of calcium to protein only if the affinities of the two sites are equal ($K_I = K_{II}$). If $\eta \neq 1$, the intensity change, which can be obtained from model calculations, will be nonlinear and the curvature will depend on both η and K_1 and K_2. The ^1H NMR data shown in Figure 10A indicate a nearly linear change in the intensities of two selected signals between 0 and 2 equiv of Ca^{2+}. In the titration of M0 with Cd^{2+}, which binds sequentially, one of these ^1H NMR

[4] We are grateful to Dr. Alwyn T. Jones, Biomedical Centre, Uppsala, Sweden, for his expert help with these experiments.

resonances (the Tyr-13 resonance at 6.77 ppm) is affected by binding of Cd^{2+} to site I only, while the other signal (the Phe-66 resonance at 6.98 ppm) is affected by Cd^{2+} entering into both sites (data not shown). In the Ca^{2+} titrations of M2 and M3 the signal at 6.77 ppm responds to Ca^{2+} entering into site I only, while the signal at 6.98 ppm is affected by binding of Ca^{2+} to both sites. In view of this we conclude that the ^1H NMR signal at 6.77 ppm in M0 responds to calcium entering into site I only. From the intensity changes of the signal at 6.77 ppm and from model calculations, we can estimate that the K_{II}/K_I ratio lies between 1 and 3, resulting in limits of $\Delta\Delta G$ of −4.7 and −5.5 kJ·mol^{-1}, respectively.

As discussed above, the ^1H NMR spectra of M0 and M4 (Tyr-13 → Phe) reveal no structural differences between the two proteins. However, removal of the hydrogen bond Tyr-13–Glu-35 has observable effects on the thermal stability of calbindin as can be seen in the temperature variation of the chemical shifts from the most high field shifted phenylalanine resonance in M0 and M4.

One would expect the removal of this intramolecular hydrogen bond which is close to site I to have some effect on the Ca^{2+}-binding properties of the protein, in particular if this hydrogen bond is present only in the Ca^{2+}-loaded form and contributes significantly to the free energy of Ca^{2+} binding. The equilibrium parameters of the two proteins M0 and M4 are, however, strikingly similar as can be seen in Tables I and II and Figure 6A, which indicate that the hydrogen bond might be formed already in the apo form. The overall appearance of the Quin2 fluorescence curves is given by the product of K_1 and K_2 and differs very little between M0 and M4. This means that the free energy change between apoprotein and calcium-loaded protein is approximately the same for both. However, this free energy of Ca^{2+} binding is divided differently between the two stoichiometric steps in M0 and M4. For M0 K_2 is greater than K_1, while the reverse relation holds for M4. This leads to the small but significant and highly reproducible difference in the fine structure of the curves, such that the S shape is less pronounced for M4 as compared to M0. The fact that the affinity of the first calcium ion has increased in M4, i.e., K_1 ($=K_I + K_{II}$) is greater in M4 than in M0, means that either K_I or K_{II} or both have increased.

Complementary information can be obtained from a Ca^{2+} titration of M4 followed by ^1H NMR. As can be seen in Figure 10B, the intensities of the two selected ^1H NMR signals do not change linearly with Ca^{2+} addition as in the case of M0. This nonlinearity can arise only if the two sites are different ($K_I \neq K_{II}$). Assuming that the intensity of the Phe-63 resonance at 6.82 ppm responds to Ca^{2+} entering into site II only, as was seen for M2 and M3, η could be obtained from model calculations, with K_1 and K_2 fixed to the values obtained from the Quin2 fluorescence data. We can estimate that η ($= K_{II}/K_I$) is greater than 5, resulting in a lower limit of $-\Delta\Delta G$ of 3.9 kJ·mol^{-1}, while no upper limit can be set in this case. We can thus conclude that even though there are significant differences between the macroscopic binding constants of M0 and M4, there is no evidence for a difference in $\Delta\Delta G$. The other resonance shown in Figure 10B (the Phe-66 resonance at 6.98 ppm) seems to be affected by Ca^{2+} entering into both sites, but not necessarily to the same extent, resulting in a flatter curve than for the Phe-63 resonance at 6.82 ppm.

Combination of K_1 and K_2 (cf. Table I) with η yield all four site binding constants of M0 and M4 as follows:[5] for M0, $K_I = (8 \pm 3) \times 10^7$ M^{-1}, $K_{II} = (1.4 \pm 0.3) \times 10^8$ M^{-1}, $K_{I,II} = (6.2 \pm 1.3) \times 10^8$ M^{-1}, and $K_{II,I} = (1.1 \pm 0.4) \times 10^9$ M^{-1}; for M4, $K_I \leq 6 \times 10^7$ M^{-1}, $K_{II} \geq 3 \times 10^8$ M^{-1}, $K_{I,II} \leq 3 \times 10^8$ M^{-1}, and $K_{II,I} \geq 1.5 \times 10^9$ M^{-1}. We thus conclude that the substitution Tyr-13 → Phe causes K_{II} to increase by a factor of about 2 or more, while there is no evidence for a change in K_I. Herzberg and James (1985a,b) have proposed, on the basis of X-ray diffraction analysis of troponin C, that the interhelix angle of an EF site changes upon Ca^{2+} binding. The hydrogen bond between Tyr-13 and Glu-35 might function as a spring such that when calcium is bound to site II the interhelix angle of site I moves toward the angle of the calcium-liganded state. Removal of this hydrogen bond might then allow the Ca^{2+} affinity for site II to increase.

The site binding constants K_I and K_{II} of M1, M2, and M3 differ enough to make the Ca^{2+} binding sequential. This means that the determined values of K_1 and K_2 correspond to K_{II} and $K_{I,II}$, respectively. We can thus conclude that the alterations in site I have little effect on the Ca^{2+} affinity of site II. The ^{113}Cd shift displacements $\delta\Delta_{II,I}$ show that there are site–site interactions also in M1, M2, and M3, although the sequential Ca^{2+} binding makes it impossible to determine $\Delta\Delta G$ (Klotz & Hunston, 1979).

The rates of binding of Ca^{2+} (k_{on}) to calbindin may be determined from the equilibrium constants and the rates of dissociation (k_{off}) where available. The k_{on} values for Ca^{2+} binding to site I are calculated to be about 3×10^9 s^{-1}·M^{-1} for mutants M1, M2, and M3. For M0 and M4 we can at present only say that the on-rates cannot exceed 3×10^9 s^{-1}·M^{-1}. These values are of the same order of magnitude as has been inferred for Ca^{2+} binding to calmodulin under low ionic strength conditions (Forsén et al., 1986). The on-rates to the pseudo-EF-hand site of the calbindins may seem very high considering the fact that the off-rate of the coordinated water would limit the on-rate to the protein to 5×10^8 s^{-1}·M^{-1} (Diebler et al., 1969). It has however been noted by Szebenyi and Moffat (1986) that the region of bovine calbindin in which the two Ca^{2+}-binding sites are located has a net charge of −7. This would certainly result in a strong attraction of an approaching divalent cation and the formation of an outer-sphere complex, explaining an observed on-rate that is higher than the off-rate of the coordinated water. Studies aimed at iluminating the role of these negative charges in calbindin have been initiated.

Thermochemical Properties. The thermochemical results presented in Table II show several interesting features. With the exception of M1, the $\Delta H°$ values for the binding of Ca^{2+} to site II in each protein are all around −8 kJ·mol^{-1}. This value is virtually the same as that found for the binding of Ca^{2+} to each site in calmodulin (Forsén et al., 1986) under similar, low ionic strength conditions. Data are available for several other calcium-binding proteins, including some with EF-hand sites, but comparisons with the results presented here are complicated by the fact that all the other measurements were made under high ionic strength conditions (Buchanan et al., 1986).

As has been pointed out (Buchanan et al., 1986), the entropy of solvation of a gaseous Ca^{2+} ion is −254 J·K^{-1}·mol^{-1}. Thus the loss of hydration water of the Ca^{2+} ion upon binding will make a major contribution to ΔS. The exceptionally low ΔS value for Ca^{2+} binding to M1 may be a result of more than one water being liganded to Ca^{2+} in site I. It is also possible that a loss of conformational entropy upon Ca^{2+} binding to the protein is one of the reasons for the generally low values of ΔS.

[5] Note that the values of the site binding constants are connected such that an increase in K_{II} and $K_{II,I}$ leads to a decrease in K_I and $K_{I,II}$ and vice versa.

The most dramatic effects on the enthalpy changes are seen for M2 and M3. Here the binding to site II is exothermic but that to site I it is endothermic, the first time a change of sign in ΔH has been observed for Ca^{2+} binding to one and the same protein. The positive ΔH values for M2 and M3 are a dominating factor in the lower Ca^{2+} affinity of the modified site I in M2 and M3 in comparison with M0, M1, and M4. By contrast, the lower Ca^{2+} affinity of the modified site in M1 is due to a reduction in ΔS that more than compensates for a more negative value of ΔH.

Conclusions

The biophysical studies described in this work show that the calbindin molecule in solution has a remarkable tolerance with respect to modifications in the Ca^{2+}-binding loop of site I. Structural changes induced appear to be primarily localized in the region modified with hardly any effects on the second Ca^{2+} site (site II) and only minor effects on the global structure. The structural stability of site II with respect to amino acid modifications at site I is paralleled also in the near constancy of dynamic and equilibrium properties pertinent to site II.

Cooperative Ca^{2+} binding in M0 and M4 has been established through the values of the two macroscopic Ca^{2+}-binding constants, K_1 and K_2, which could be determined with good accuracy. The observed localized changes in the properties of mutant calbindins and the appearance of sequential Ca^{2+} ion binding in some of the mutant proteins have allowed the identification of ^1H NMR resonances that primarily respond to binding of Ca^{2+} to one of the sites. This has in turn permitted us to estimate the ratios between the site bindig constants K_{II} and K_I in M0 and M4—the two proteins in which cooperative Ca^{2+} binding is demonstrated. From the K_{II}/K_I ratios and the macroscopic binding constants it has been possible to assess, within narrow limits, the free energy of interaction, $\Delta\Delta G$, between the two Ca^{2+} sites (for M0, $\Delta\Delta G = -5.1 \pm 0.4$ kJ·mol^{-1}; for M4, $\Delta\Delta G < -3.9$ kJ·mol^{-1}).

The present study has illustrated the synergistic effects of applying several different biophysical methods to the same set of mutant proteins.

Acknowledgments

We thank Cecilia Nilsson at Tecator AB, Höganäs, Sweden, for the micro-Kjeldahl analyses, Doletha Szebenyi, Cornell University, for help with the figures, Theo Hofmann, Toronto, for valuable discussion and for providing antisera and porcine calbindin, and Per Linse, Lund, Sweden, for computational advice.

Registry No. Ca, 7440-70-2.

References

Babu, Y. S., Sack, J. S., Greenhough, T. G., Bugg, C. E., Means, A. R., & Cook, W. J. (1985) *Nature (London) 315*, 37–40.

Belton, P. S., Cox, I. Y., & Harris, R. K. (1985) *J. Chem. Soc., Faraday. Trans. 2 81*, 63–75.

Brodin, P., Grundström, T., Hofmann, T., Drakenberg, T., Thulin, E., & Forsén, S. (1986) *Biochemistry 25*, 5371–5377.

Bryant, D. T. W. (1985) *Biochem. J. 226*, 613–616.

Buchanan, J. D., Corbett, R. J. T., & Roche, R. S. (1986) *Biophys. Chem. 23*, 183–199.

Chen, A.-T., & Wadsö, I. (1982) *J. Biochem. Biophys. Methods 6*, 307–316.

Chiancone, E., Thulin, E., Boffi, A., Forsén, S., & Brunori, M. (1986) *J. Biol. Chem. 261*, 16306–16308.

Dalgarno, D. C., Levine, B. A., Williams, R. J. P., Fullmer, C. S., & Wasserman, R. H. (1983) *Eur. J. Biochem. 137*, 523–533.

Diebler, H., Eigen, M., Ilgenfrotz, G., Maass, G., & Winkler, R. (1969) *Pure Appl. Chem. 20*, 93–115.

Drakenberg, T., Forsén, S., & Lilja, H. (1983) *J. Magn. Reson. 53*, 412–422.

Forsén, S., Vogel, H., & Drakenberg, T. (1986) in *Calcium and Cell Function* (Cheung, W. Y., Ed.) Vol. 6, pp 113–157, Academic, New York.

Forsén, S., Drakenberg, T., Thulin, E., Brodin, P., Grundström, T., Linse, S., Sellers, P., & Elmdén, K. (1987) in *Calcium Binding Proteins in Health & Disease* (Norman, A. W., et al., Ed.) Academic, New York (in press).

Fullmer, C. S., & Wasserman, R. H. (1981) *J. Biol. Chem. 256*, 5669–5674.

Harris, T. (1982) *Nature (London) 299*, 298–299.

Herzberg, O., & James, M. N. G. (1985a) *Biochemistry 24*, 5298–5302.

Herzberg, O., & James, M. N. G. (1985b) *Nature (London) 313*, 653–659.

Herzberg, O., Moult, J., & James, M. N. G. (1986) *J. Biol. Chem. 261*, 2638–2644.

Hofmann, T., Kawakami, M., Hitchman, A. J. W., Harrison, J. E., & Dorrington, K. J. (1979) *Can. J. Biochem. 57*, 737–748.

Johansson, B. G. (1972) *Scand. J. Clin. Lab. Invest. 29, Suppl. No. 124*, 7–19.

Karlsson, R., & Kullberg, L. (1976) *Chem. Scr. 9*, 54–57.

Klee, C. B., & Vanaman, T. C. (1982) *Adv. Protein Chem. 35*, 214–321.

Klotz, I. M., & Hunston, D. I. (1979) *Arch. Biochem. Biophys. 193*, 314–328.

Kretsinger, R. H., & Nockolds, C. E. (1973) *J. Biol. Chem. 248*, 3313–3326.

Kretsinger, R. H., & Weissman, L. J. (1986) *J. Inorg. Biochem. 28*, 289–302.

Manalan, A. S., & Klee, C. B. (1984) *Adv. Cyclic Nucleotide Protein Phosphorylation Res. 18*, 227–278.

McCubbin, W. D., & Kay, C. M. (1980) *Acc. Chem. Res. 13*, 185–192.

Moews, P. C., & Kretsinger, R. H. (1975) *J. Mol. Biol. 91*, 201–228.

Morishima, I., Kurono, M., & Shiro, Y. (1986) *J. Biol. Chem. 261*, 9391–9399.

Morton, R. W., Chung, J. K., Miller, J. L., Charlton, J. P., & Fager, R. S. (1986) *Anal. Biochem. 157*, 345–352.

Öjelund, G., & Wadsö, I. (1968) *Acta Chem. Scand. 22*, 2691–2699.

Potter, J. D., & Johnson, J. D. (1982) in *Calcium and Cell Function* (Cheung, W. Y., Ed.) Vol. 2, pp 145–173, Academic, New York.

Rasmussen, H. (1986a) *N. Engl. J. Med. 314*, 1094–1101.

Rasmussen, H. (1986b) *N. Engl. J. Med. 314*, 1164–1170.

Seamon, K. B., & Kretsinger, R. H. (1983) in *Metal Ions in Biology* (Spiro, T., Ed.) Vol. 6, pp 1–52, Wiley-Interscience, New York.

Smith, M. (1982) *Trends Biochem. Sci. (Pers. Ed.) 7*, 440–442.

Sundralingam, M., Bergstrom, R., Strasburg, G., Rao, S. T., Roychowdhury, P., Greaser, M., & Wang, B. C. (1985) *Science (Washington, D.C.) 227*, 945–948.

Szebenyi, D. M. E., & Moffat, K. (1983) in *Calcium Binding Proteins* (de Bernard, B., Ed.) pp 199–205, Elsevier, New York.

Szebenyi, D. M. E., & Moffat, K. (1986) *J. Biol. Chem. 261*, 8761–8777.
Szebenyi, D. M. E., Obendorf, S. F., & Moffat, K. (1981) *Nature (London) 294*, 327–332.
Tsai, M.-D., Drakenberg, T., Thulin, E., & Forsén, S. (1987) *Biochemistry 26*, 3635–3643.
Vogel, H. J., & Forsén, S. (1987) in *Biological Magnetic Resonance* (Berliner, L. J., & Reuben, J., Eds.) Plenum, New York (in press).
Vogel, H. J., Drakenberg, T. D., Forsén, S., O'Neil, J. D. J., & Hoffmann, T. (1985) *Biochemistry 24*, 3870–3876.
Wasserman, R. H., & Fullmer, C. S. (1982) in *Calcium and Cell Function* (Cheung, W. Y., Ed.) Vol. 2, pp 175–216, Academic, New York.
Wasserman, R. H., Fullmer, C. S., & Taylor, A. N. (1978) in *Vitamin D* (Lawson, E. E. M., Ed.) pp 133–166, Academic, New York.
Weber, G. (1975) *Adv. Protein Res. 29*, 1–83.

Nucleotide Sequence and Organization of the Human S-Protein Gene: Repeating Peptide Motifs in the "Pexin" Family and a Model for Their Evolution

Dieter Jenne*,‡,§ and Keith K. Stanley§

Institute of Medical Microbiology, Justus-Liebig-University in Giessen, 6300 Giessen, FRG, and European Molecular Biology Laboratory, 6900 Heidelberg, FRG

Received March 11, 1987; Revised Manuscript Received June 4, 1987

ABSTRACT: The S-protein/vitronectin gene was isolated from a human genomic DNA library, and its sequence of about 5.3 kilobases including the adjacent 5′ and 3′ flanking regions was established. Alignment of the genomic DNA nucleotide sequence and the cDNA sequence indicated that the gene consisted of eight exons and seven introns. The intron positions in the S-protein gene and their phase type were compared to those in the hemopexin gene which shares amino acid sequence homologies with transin and the S-protein. Three introns have been found at equivalent positions; two other introns are very close to these positions and are interpreted as cases of intron sliding. Introns 3–7 occur at a conserved glycine residue within repeating peptide segments, whereas introns 1 and 2 are at the boundaries of the Somatomedin B domain of S-protein. The analysis of the exon structure in relation to repeating peptide motifs within the S-protein strongly suggests that it contains only seven repeats, one less than the hemopexin molecule. A very similar repeat pattern like that in hemopexin is shown to be present also in two other related proteins, transin and interstitial collagenase. An evolutionary model for the generation of the repeat pattern in the S-protein and the other members of this novel "pexin" gene family is proposed, and the sequence modifications for some of the repeats during divergent evolution are discussed in relation to known unique functional properties of hemopexin and S-protein.

Several biological functions have been ascribed to a single 75-kilodalton (kDa)[1] glycoprotein of human plasma (Jenne & Stanley, 1985). In serum culture media, this protein, called vitronectin or serum spreading factor, is the principal agent mediating the adhesion and spreading of cells and facilitating their proliferation on surfaces in vitro (Barnes et al., 1980; Hayman et al., 1985). When complement is activated, the same protein, called complement S-protein, participates in the fluid phase assembly of the terminal complement proteins to form the soluble SC5b-9 complex; however, it is not found in the C5b-9 membrane complex that is assembled only on a lipid bilayer and generates transmembrane channels (Kolb & Müller-Eberhard, 1975; Bhakdi et al., 1976; Bhakdi & Tranum-Jensen, 1983). S-Protein incorporation into nascent C5b-7 complexes prevents their membrane attachment and the formation of cytolytically active complement complexes on lipid membranes after successive addition of C8 and C9. Therefore, S-protein/vitronectin appears to protect innocent bystander cells from membrane damage by nascent complement complexes (Podack et al., 1977, 1978).

S-Protein also forms stable ternary complexes with antithrombin III and thrombin during thrombin inactivation. It binds through a cryptic site in antithrombin III and exerts a net protective effect on thrombin toward its inactivation by the inhibitor (Jenne et al., 1985a; Ill & Ruoslahti, 1985). The molecule further possesses a heparin and glycosaminoglycan binding site (residues 348–380) (Suzuki et al., 1984) which is not exposed in the native plasma protein (Hayashi et al., 1985; Barnes et al., 1985). Binding to heparin-like molecules contributes to its procoagulatory role in the clotting process (Preissner et al., 1985).

The Arg-Gly-Asp (R-G-D) peptide sequence of S-protein/vitronectin (residues 45–47) interacts specifically with a cell surface receptor, the vitronectin receptor (Pytela et al., 1985). The molecule can therefore function as a cross-linker between cells and the extracellular matrix by virtue of its two different binding sites.

S-Protein has evidently specialized for a variety of binding functions which reside in different regions of the protein.

* Address correspondence to this author at the Institut de Biochimie, Université de Lausanne, CH-1066 Epalinges, Switzerland. Supported in part by a fellowship from the European Molecular Biology Organization.
‡ Justus-Liebig-University in Giessen.
§ European Molecular Biology Laboratory.

[1] Abbreviations: SDS, sodium dodecyl sulfate; HTF, *Hpa*II tiny fragments; CAT, chloramphenicol acetyltransferase; NaH_2PO_4, sodium dihydrogen orthophosphate; pEX, expression plasmid (Stanley & Luzio, 1984); kDa, kilodalton(s); bp, base pair(s); TK, thymidine kinase; kb, kilobase(s).

0006-2960/87/0426-6735$01.50/0